

Rheology of high speed granular flows in presence and absence of air

Satyabrata Patro^{1,*}, Tarun De^{2,**}, and Anurag Tripathi^{3,***}

¹R&D Tata Steel limited, Jamshedpur, Jharkhand, India

²Department of Chemical Engineering, Indian Institute of Technology Kanpur, Kanpur, Uttar Pradesh, India

³Department of Chemical Engineering, Indian Institute of Technology Kanpur, Kanpur, Uttar Pradesh, India

Abstract. The rheology of granular materials at large inertial numbers ($I \geq 1$) exhibits a non-monotonic variation of the effective friction coefficient $\mu(I)$, as shown by Patro et al. (2021, 2023). These studies highlight the need to account for the non-monotonic behavior of $\mu(I)$, the dilatancy law linking solids fraction (ϕ) to I , and stress anisotropy via a normal stress difference law to accurately predict flow properties in rapid granular flows. While this inertial number-based rheology successfully describes both dense and dilute flow regimes, most simulations neglect the presence of air, despite its non-negligible drag in high-speed flows. This raises questions about the applicability of simulation findings to real-world scenarios. We conducted CFD-DEM simulations of 1mm, slightly polydisperse, inelastic, frictional spheres flowing over a bumpy chute at a high inclination ($\theta = 38^\circ$), using LIGGGHTS for DEM (no air) and CFDEM coupled with OpenFOAM (with air). Air is modeled as an incompressible Newtonian fluid with drag based on the Di Felice model. Results show that air reduces grain velocity v_x , slightly increases ϕ , and lowers the steady-state inertial number I . We analyze how air alters $\mu(I)$, $\phi(I)$, and normal stress differences, emphasizing its role in high-speed granular flows.

1 Introduction

Granular materials are commonly seen in many geophysical flows such as avalanches, debris flow, and landslides, as well as in many solids handling industries. The complex flow behavior based on particle-particle and particle-environment interactions has gained popularity over the past few decades, aimed at developing predictive rheological models. Jop et.al [2] proposed a three-dimensional generalization of the friction law in tensorial form—a viscoplastic model linking the effective friction coefficient μ to the inertial number I popularly known as the JFP model. The inertial number is a dimensionless number that characterizes the flow regimes in granular materials and is defined as

$$I = \frac{d\dot{\gamma}}{\sqrt{P/\rho_p}} \quad (1)$$

where d and ρ_p are the particle diameter and particle density, respectively. $\dot{\gamma}$ is the local shear rate; and P is the confining pressure. The JFP model suggests that the effective friction coefficient increases with increasing inertial number and saturates at large values of I . Borzsonyi et. al. [3] performed DEM simulations of flow over a chute and showed a decrease in the effective friction coefficient at large inertial numbers. Holyoake et. al. [5] performed experiments and reported a similar non-monotonic variation of $\mu(I)$ at high inclinations. Such non-monotonic variation of $\mu(I)$ has also been reported using data from chute flows

and plane shear flows by Mandal et. al. [6, 7]. These authors proposed a modification to the JFP model to capture this non-monotonic variation of μ with I [6, 7]. None of these studies, however, considered the effect of normal stress differences. A recent study by Patro et. al. [8, 9] shows a non-monotonic variation of the effective friction coefficient $\mu(I)$ at large inertial numbers I . Notably, most studies dealing with granular flows at high inertial numbers ignore the presence of air in the simulations. However, in the case of rapid granular flows, the air drag on particles no longer remains negligible due to the high particle speeds. Hence, it is not clear whether the simulation findings for granular flows at large inertial numbers can be extended to real-life, high-speed granular flows on Earth. In this work, we perform CFD-DEM simulations of slightly polydisperse, inelastic, frictional spheres of 1 mm size flowing over a chute with a bumpy base, neglecting the effect of side walls. The results from the DEM simulations demonstrate that including the effect of air as the medium between grains leads to a reduction in particle velocity and a slight increase in solids fraction. The steady-state inertial number in the presence of air is slightly smaller compared to the case ignoring air. We also discuss how the variation of the effective friction coefficient, solids fraction, and normal stress differences with the inertial number is affected by the presence of air.

2 Simulation Methodology

The granular flow over a rough inclined plane was simulated using a coupled approach combining the Discrete El-

*e-mail: satyabrata.patro1@tatasteel.com

**e-mail: talk2tarunde@gmail.com

***e-mail: anuragt@iitk.ac.in

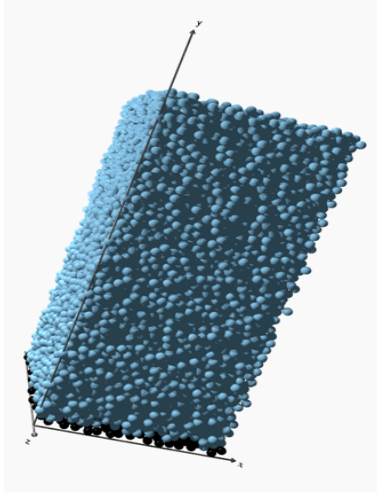


Figure 1. Chute flow simulation setup of dimensions $20d \times 40d \times 20d$. Blue spheres represent the moving particles, while black spheres represent the static particles used to create the bumpy base. Periodic boundary conditions are used in the flow (x) and vorticity (z) directions.

ement Method (DEM) for particle interactions and Computational Fluid Dynamics (CFD) to account for air drag effects where applicable. The DEM simulations were performed using the Hertz-Mindlin contact model, while the CFD component incorporated the De Felice model to capture fluid-particle interactions. In the DEM simulations, the simulation domain had dimensions of $20d \times 40d \times 20d$, with d representing the mean particle diameter. The length and width of the simulation box were both set to $20d$, and periodic boundaries were applied along the x - and z - directions (flow and vorticity directions). The inclination angle of the plane was set to a high value of $\theta \sim 38^\circ$ to study the flow behavior at large inertial numbers ($I \geq 1$), both in the presence and absence of an interstitial fluid medium (chosen to be air). The restitution coefficient e_n and the coefficient of static friction μ were set to 0.5. We used LIGGGHTS, an open-source DEM software, to simulate granular flow in the absence of air. The CFD-DEM simulations, incorporating air effects, were performed using LIGGGHTS interfaced with OpenFOAM via CFDEM coupling. The air phase was modeled as an incompressible Newtonian fluid in OpenFOAM, and the solids volume-fraction-dependent drag force on the particles was accounted for using the Di-Felice drag model. The following subsections provide further methodological details.

2.1 Hertz-Mindlin Model

In this model, the net force $|\vec{F}|$ acting on a particle due to contact with another particle is given as:

$$|\vec{F}_n| = \frac{4}{3} Y_{eff} \sqrt{r_{eff}} \delta_n^{3/2} - 2 \sqrt{\frac{5}{6}} \alpha m_{eff}^{1/2} \sqrt{2} Y_{eff}^{1/2} \delta_n^{1/4} v_n \quad (2)$$

$$|\vec{F}_t| = -8 G_{eff} \delta_n^{3/2} \sqrt{r_{eff}} \delta_t - 2 \sqrt{\frac{5}{6}} \alpha m_{eff}^{1/2} \sqrt{2} G_{eff}^{1/2} \delta_n^{1/4} v_t \quad (3)$$

Equations (2) and (3) contribute to the magnitudes of the normal and tangential forces, respectively, acting on a particle whenever it comes into contact with another particle. Here, δ_n and δ_t are the overlaps in the normal and tangential directions, respectively, and v_n and v_t are the magnitudes of the relative velocity of impact in the normal and tangential directions. The simulation time step Δt is chosen to satisfy $\Delta t \leq 0.15 t_{Rayleigh}$, where

$$t_{rayleigh} = \frac{\pi r_{eff} \sqrt{(\rho_p / G_{eff})}}{(0.1631\nu + 0.8766)} \quad (4)$$

2.2 De Felice Model Accounting for Air Drag

To investigate the influence of air drag, a CFD approach was coupled with the DEM framework using the De Felice model to compute fluid-particle interactions. The Di Felice drag model is a semi-empirical correlation that calculates the drag force on a particle in a fluid while considering the effects of neighboring particles (i.e., particle volume fraction or voidage). It is particularly useful for fluidized beds, granular flows, and other systems where particles are immersed in a fluid. It can also handle laminar flow conditions when the particle Reynolds number is low. The drag force (\mathbf{F}_d) acting on a single particle in the Di Felice model is given by:

$$\mathbf{F}_d = \frac{1}{2} C_D \rho_f \pi \frac{d_p^2}{4} |\mathbf{u}_f - \mathbf{u}_p| (\mathbf{u}_f - \mathbf{u}_p) \varepsilon^{2-\chi} \quad (5)$$

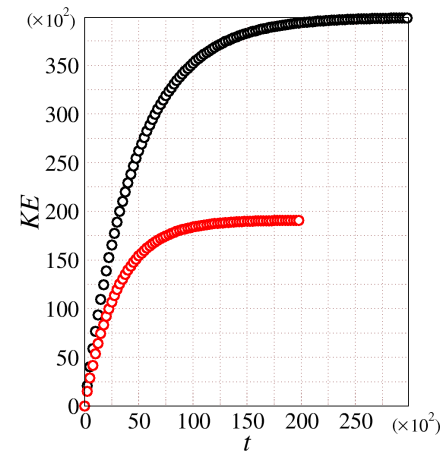


Figure 2. Variation of the kinetic energy with time comparing cases with drag (red symbols) and without air drag (black symbols). The chute inclination is $\theta = 38^\circ$ from the horizontal.

where (C_D) is the drag coefficient, ρ_f is the fluid density, d_p is the particle diameter, \mathbf{u}_f is the fluid velocity vector, \mathbf{u}_p is the particle velocity, ε is the voidage (fluid volume fraction, dimensionless; ($0 < \varepsilon \leq 1$)), and χ is the voidage exponent, which depends on the particle Reynolds number.

3 Results

We present DEM simulation results for the flow of spheres over a bumpy inclined surface inclined at $\theta = 38^\circ$, starting

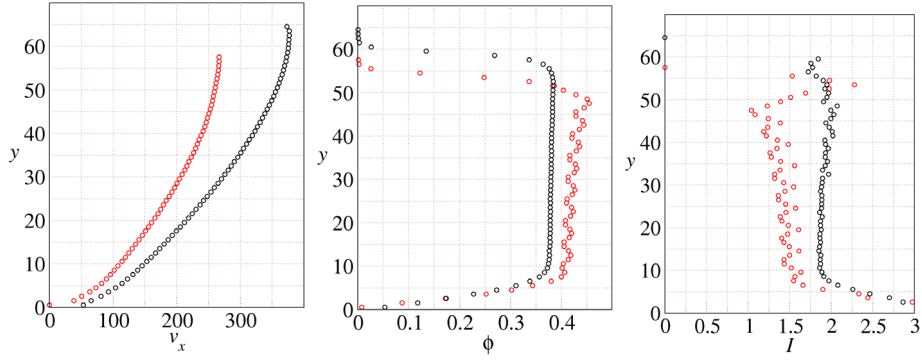


Figure 3. Variation of velocity v_x , solids fraction ϕ and inertial number I with height y from the base, for $e_n = 0.5$, accounting for the effect of air drag (with and without). The chute inclination is $\theta = 38^\circ$.

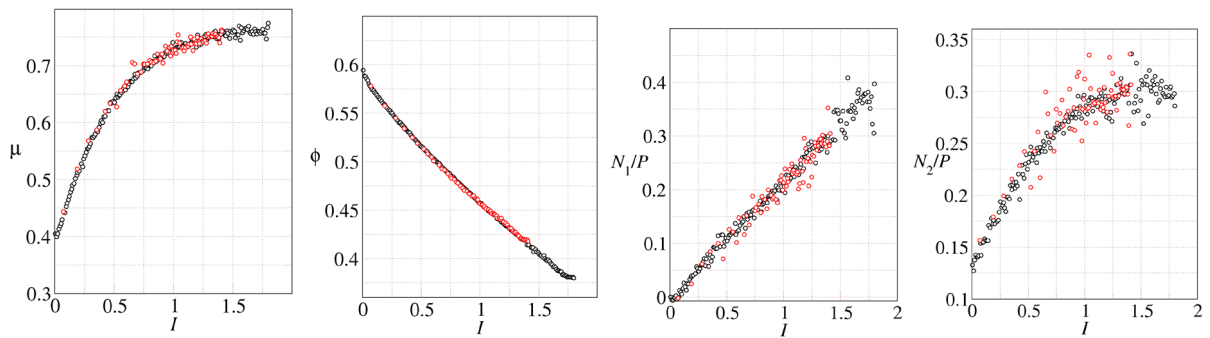


Figure 4. Variation of the effective friction coefficient μ , solids fraction ϕ , first normal stress difference to pressure ratio (N_1/P), and second normal stress difference to the pressure ratio (N_2/P) with the inertial number I for $e_n = 0.5$, showing the effect of air drag (with and without).

from a settled layer height of $L_y = 40d$, for restitution coefficient $e_n = 0.5$, where d is the mean particle diameter. The coefficient of static friction between the particles is $\mu = 0.5$. All quantities reported are non-dimensionalized using d , m , $\sqrt{d/g}$ and mg as the characteristic length, mass, time, and force units, respectively, where m is the mass of the particle having diameter d , and g is the gravitational acceleration.

Figure 2 shows the time evolution of average kinetic energy for a system of spherical particles flowing over a rough inclined plane inclined at $\theta = 38^\circ$. The simulation begins from an initial settled state. As evident, with increasing time, the kinetic energy increases due to gravitational acceleration along the incline, eventually reaching a steady state where the energy gained is balanced by dissipative losses from particle collisions and friction. We compare two cases: 1. Considering the interstitial medium as air (shown as red symbols), and 2. Without considering any interstitial medium (shown as black symbols). The maximum kinetic energy in the absence of air drag exceeds that with air drag, reflecting the additional dissipation introduced by aerodynamic resistance.

Fig. 3(a) shows the velocity v_x with height from the chute base y for spherical particles flowing over a chute in-

clined at $\theta = 38^\circ$. The velocity profile was observed to follow a Bagnold-type profile, i.e., $v_x \sim y^{3/2}$, consistent with earlier observations in 2D studies of flow over an inclined plane at large inertial numbers by Patro et.al. [9]. Bagnold's theoretical velocity profile is in very good agreement with the DEM simulation results for a wide range of inclination angles and restitution coefficients. A detailed analysis of 3D flow of spheres is presented in the thesis [10]. For the case without air drag, the profile exhibits a higher v_x across all heights compared to the case with air drag, reflecting the additional dissipative effect of resistance. Fig. 3(b) shows the solids fraction ϕ with height from the base y , for an inclination angle $\theta = 38^\circ$. The solids fraction is nearly constant in most of the bulk layer and decreases toward the free surface and close to the base. The presence of air drag slightly increases the solids fraction ϕ , as reduced velocities enhance particle settling. The profile without air drag shows a marginally lower packing density due to higher velocity. Fig. 3(c) shows the variation of the inertial number I with height from the base y (for an inclination angle $\theta = 38^\circ$). The case without air drag yields a higher inertial number throughout the bed owing to the greater velocities, while air drag suppresses the inertial number by reducing particle momentum.

In Figure 4, we report the variation of the effective friction coefficient μ , solids fraction ϕ , the ratio of first normal stress difference to pressure N_1/P , and the ratio of second normal stress difference to pressure N_2/P with inertial number I for $e_n = 0.5$. The effective friction coefficient obtained from simulations without air drag increases up to $I \approx 1.8$ and shows saturating behavior at large inertial numbers. However, the effective friction coefficient obtained from the simulations with air drag increases up to $I \approx 1.38$ and also shows a saturating trend at large inertial numbers. While the current 3D simulations with air drag exhibit signs of saturation in the effective friction coefficient μ at large inertial numbers, further exploration at higher inclination angles (greater than 38°) could provide deeper insights into this saturation behavior. At steeper inclinations, the system approaches a transition from dense to dilute flow regimes, as the solids fraction ϕ decreases to approximately $\phi \sim 0.3$ (see Fig. 4(b)). Simulations under such conditions become increasingly expensive due to high particle velocities and reduced solids fraction, which require smaller time steps to accurately capture the flow dynamics. The variation of solids fraction is plotted with the inertial number in Fig. 4(b). In Fig. 4(c), we report the variation of the ratio of the first normal stress difference to pressure (N_1/P) with the inertial number I . We also report the variation of the ratio of the second normal stress difference to pressure (N_2/P) with the inertial number I .

4 Conclusion

We performed DEM simulations to investigate the flow of grains over a rough inclined plane inclined at $\theta = 38^\circ$. The influence of air drag on granular flow dynamics was studied across a range of properties, including kinetic energy, steady-state flow profiles, and rheological characteristics of granular materials. The presence of air drag significantly reduces the maximum kinetic energy and slightly delays the attainment of steady state compared to the case without drag, underscoring its role as an additional dissipative mechanism. Steady-state profiles further confirm these dissipative effects: the velocity profile exhibited Bagnold-type scaling with a basal slip velocity. Correspondingly, the solids fraction increased slightly near the base in the presence of air drag, reflecting enhanced particle settling. The inertial number was consistently lower with air drag, indicating a shift toward a less inertia-dominated regime.

The rheological analysis provided deeper insights into the granular flow's constitutive behavior. The effective

friction coefficient increased with the inertial number, with the case without air drag exhibiting higher values due to greater particle momentum and reduced dissipation. Similarly, the solids fraction decreased with increasing inertial number, though air drag moderated this trend by promoting denser packing at lower velocities. These insights are particularly relevant for high-inclination flows where slip and inertial effects dominate, offering a refined understanding of dissipation mechanisms in granular systems. Future work could explore the sensitivity of these findings to particle size, air drag models, or inclination angles to further generalize the role of aerodynamic interactions in granular rheology.

References

- [1] L.E. Silbert, D. Ertas, G.S. Grest, T.C. Halsey, D. Levine, and S.J. Plimpton, Granular flow down an inclined plane: Bagnold scaling and rheology. *Phys. Rev. E.* **64.5**, 051302 (2001).
- [2] P. Jop, Y. Forterre, and O. Pouliquen, A constitutive law for dense granular flows. *Nature* **441.7094**, 727–730 (2006).
- [3] T. Börzsönyi, R. Ecke and J.N. McElwaine, Patterns in Flowing Sand: Understanding the Physics of Granular Flow. *Phys. Rev. Lett.* **103**, 178302 (2009).
- [4] A. Tripathi and D.V. Khakhar, Rheology of binary granular mixtures in the dense flow regime. *Phys. Fluids* **23.11**, 113302 (2011).
- [5] A.J. Holyoake and J.N. McElwaine, High-speed granular chute flows. *Journal of Fluid Mechanics* **710**, 35–71 (2012).
- [6] S. Mandal and D.V. Khakhar, A study of the rheology of planar granular flow of dumbbells using discrete element method simulations. *Phys. Fluids* **28.10**, 103301 (2016).
- [7] S. Mandal and D.V. Khakhar, A study of the rheology and micro-structure of dumbbells in shear geometries. *Phys. Fluids* **30.1**, 013303 (2018).
- [8] S. Patro, A. Tripathi, S. Kumar, and A. Majumdar, Unsteady granular chute flows at high inertial numbers. *Phys. Rev. Fluids* **8**, 8, 124303 (2023).
- [9] S. Patro, M. Prasad, Ayushi Tripathi, P. Kumar, A. Tripathi, Rheology of two-dimensional granular chute flows at high inertial numbers. *Phys. Fluids* **33 (11)**, 113321 (2021).
- [10] S. Patro, Unified Rheology for dense and dilute granular flows. *Doctoral dissertation, IIT Kanpur*(2024).